Received: 15 December 2017 | Revised: 8 September 2018 | Accepted: 10 September 2018

DOI: 10.1111/gcb.14457

PRIMARY RESEARCH ARTICLE

WILEY Global Change Biology

Windthrows control biomass patterns and functional composition of Amazon forests

Daniel Magnabosco Marra[1,2,3] | Susan E. Trumbore[1] | Niro Higuchi[2] | Gabriel H. P. M. Ribeiro[2] | Robinson I. Negrón-Juárez[4] | Frederic Holzwarth[3] | Sami W. Rifai[5] | Joaquim dos Santos[2] | Adriano J. N. Lima[2] | Valdely F. Kinupp[6] | Jeffrey Q. Chambers[4,7] | Christian Wirth[3,8,9]

[1]Biogeochemical Processes Department, Max-Planck-Institute for Biogeochemistry, Jena, Germany

[2]Laboratório de Manejo Florestal, Instituto Nacional de Pesquisas da Amazônia, Manaus, Brazil

[3]AG Spezielle Botanik und Funktionelle Biodiversität, Universität Leipzig, Leipzig, Germany

[4]Climate and Ecosystem Sciences Division, Lawrence Berkeley National Laboratory, Berkeley,California

[5]Environmental Change Institute, University of Oxford, Oxford, UK

[6]Ciência e Tecnologia do Amazonas, Campus Manaus-Zona Leste, Herbário EAFM, Instituto Federal de Educação, Manaus, Brazil

[7]Geography Department, University of California, Berkeley, California

[8]German Centre for Integrative Biodiversity Research (iDiv) Halle-Jena-Leipzig, Leipzig, Germany

[9]Functional Biogeography Fellow Group, Max-Planck-Institute for Biogeochemistry, Jena, Germany

Correspondence
Daniel Magnabosco Marra, Biogeochemical Processes Department, Max-Planck-Institute for Biogeochemistry, Jena, Germany.
Email: dmarra@bgc-jena.mpg.de.

Funding information
Conselho Nacional de Desenvolvimento Científico e Tecnológico, Grant/Award Number: SAWI Project (Chamada Universal MCTI/Nu 14/2012, Proc. 473357/2), INCT Madeiras da Amazônia; Coordenação de Aperfeiçoamento de Pessoal de Nível Superior, Grant/Award Number: INCT

Abstract

Amazon forests account for ~25% of global land biomass and tropical tree species. In these forests, windthrows (i.e., snapped and uprooted trees) are a major natural disturbance, but the rates and mechanisms of recovery are not known. To provide a predictive framework for understanding the effects of windthrows on forest structure and functional composition (DBH ≥10 cm), we quantified biomass recovery as a function of windthrow severity (i.e., fraction of windthrow tree mortality on Landsat pixels, ranging from 0%–70%) and time since disturbance for *terra-firme* forests in the Central Amazon. Forest monitoring allowed insights into the processes and mechanisms driving the net biomass change (i.e., increment minus loss) and shifts in functional composition. Windthrown areas recovering for between 4–27 years had biomass stocks as low as 65.2–91.7 Mg/ha or 23%–38% of those in nearby undisturbed forests (~255.6 Mg/ha, all sites). Even low windthrow severities (4%–20% tree mortality) caused decadal changes in biomass stocks and structure. While rates of biomass increment in recovering vegetation were nearly double (6.3 ± 1.4 Mg ha^{-1} $year^{-1}$) those of undisturbed forests (~3.7 Mg ha^{-1} $year^{-1}$), biomass loss due to post-windthrow mortality was high (up to −7.5 ± 8.7 Mg ha^{-1} $year^{-1}$, 8.5 years since disturbance) and unpredictable. Consequently, recovery to 90% of "pre-disturbance" biomass takes up to 40 years. Resprouting trees contributed little to biomass recovery. Instead, light-demanding, low-density genera (e.g., *Cecropia*, *Inga*, *Miconia*, *Pourouma*, *Tachigali*, and *Tapirira*) were favored, resulting in substantial post-windthrow species turnover. Shifts in functional composition demonstrate that windthrows affect the resilience of live tree biomass by favoring soft-wooded species with shorter life spans that are more vulnerable to future disturbances. As the time required for forests to recover biomass is likely similar to the recurrence interval of windthrows triggering succession, windthrows have the potential to control landscape biomass/carbon dynamics and functional composition in Amazon forests.

Madeiras da Amazônia; Fundação de Amparo à Pesquisa do Estado do Amazonas, Grant/Award Number: INCT Madeiras da Amazônia; Max-Planck-Institut für Biogeochemistry, Grant/Award Number: Amazon Tall Tower Observatory (ATTO); National Aeronauticsand Space Administration, Grant/Award Number: Biodiversity Program Project 08-BIODIV-10

KEYWORDS
biodiversity, biomass/carbon dynamics and resilience, forest blowdowns, natural disturbances, recovery dynamics, tree mortality, tropical forest ecosystems

1 | INTRODUCTION

Natural disturbances such as windthrows (i.e., snapped and uprooted trees) impact tropical forests worldwide (Burslem, Whitmore, & Brown, 2000; Everham & Brokaw, 1996; Lugo, 2008; Mitchell, 2013; Vandermeer, la Cerda, Boucher, Perfecto, & Ruiz, 2000). In the Central and Western Amazon, there is growing evidence indicating that relatively small windthrows, ranging from few toppled trees (~400 m^2) to intermediate-sized events of several hectares, occur frequently and are a major mechanism of mortality of adult trees (Espírito-Santo et al., 2010; Negrón-Juárez et al., 2018, 2017 ; Nelson, Kapos, Adams, Oliveira, & Braun, 1994). They create a forest mosaic of differently sized patches reflecting the legacy of a disturbance regime that may trigger succession and cause spatial variation in forest structure and species composition (Chambers et al., 2013; Marra et al., 2014; Rifai et al., 2016). To our knowledge, this is the first field study investigating how windthrows have influenced subsequent patterns of biomass/carbon balance and functional composition in Amazon forests.

Windthrows in the Amazon are produced by downbursts (Garstang, White, Shugart, & Halverson, 1998; Nelson et al., 1994) and tree mortality in disturbed areas can reach in excess of 90% (Marra et al., 2014; Rifai et al., 2016). Model simulations for the Central Amazon predict the mean and median intervals between succession-inducing windthrows of ~400 m^2 to be 74 and 51 years, respectively (Chambers et al., 2013; Figure 4). Applying the same return frequency, we estimate that windthrows have affected 18% of the landscape in the last decade, and 43% in the last 50 years (Supporting Information Figure S1a). An assessment of the windthrow variability over a 12-year period (1999–2010) across the same region indicates that larger windthrows (>5 ha in size) affected 0.5% of the landscape (Negrón-Juárez et al., 2017) (Supporting Information Figure S1b). Both studies suggest that an important fraction of the forest landscape is likely to carry a legacy of wind disturbance with unknown consequences for the regional carbon balance.

Windthrows promote selective tree-mortality (Canham, Thompson, Zimmerman, & Uriarte, 2010; Curran et al., 2008; Marra et al., 2014; Rifai et al., 2016). The woody debris created may quickly decompose (e.g., after 2–46 years) (Chambers, Higuchi, Schimel, Ferreira, & Melack, 2000; Hérault et al., 2010) releasing mineralized nutrients (Vitousek & Denslow, 1986) while adding residual organic matter to the soil (dos Santos et al., 2016). Mortality of the pre-disturbance tree cohort often continues into the recovery phase, when for example, isolated survivors and resprouters suffer from mechanical and/or physiological stress induced by successive wind disturbances or changes in environmental conditions (Everham & Brokaw, 1996; Lugo, 2008; Putz & Brokaw, 1989; Schwartz et al., 2017). Mortality also occurs during recovery when the new cohort rapidly fills growing space and self-thinning commences (Scalley, Scatena, Lugo, Moya, & Estrada Ruiz, 2010; Vandermeer & Cerda, 2004).

Biomass recovery in windthrows can occur through multiple mechanisms including regeneration from seeds, recruitment of advanced regeneration, gap-filling lateral growth of surviving trees and resprouting from roots, stumps, and broken stems (Burslem & Whitmore, 1999; Mascaro et al., 2005; Putz & Brokaw, 1989; Scalley et al., 2010). Windthrows can also promote shifts in composition through species turnover (Chambers et al., 2009; Everham & Brokaw, 1996; Marra et al., 2014), often accompanied by changes in functional traits between early successional species and those dominating mature forests. Early successional species tend to be more light demanding, lower wood density, shorter lifespan, different in architecture, reduced mechanical stability and higher vulnerability to new windthrows, and other climate-induced disturbances such as drought (Baker et al., 2004; Canham et al., 2010; Laurance & Curran, 2008; Magnabosco Marra et al., 2016; Rüger et al., 2018; Swaine & Whitmore, 1988). These traits reduce the potential of forests dominated by early successional species to reach the high carbon densities (Chambers et al., 2013) and long carbon residence times of old-growth forests (Galbraith et al., 2013).

The rates of biomass recovery (i.e., the sum of processes including regrowth, recruitment, resprouting, post-windthrow mortality, and species turnover) may differ with windthrow severity, that is, with the overall tree mortality and size of gaps formed. Of special interest is how the rates of biomass recovery and species turnover compare to the mean return interval of windthrow disturbance. If these are rapid compared to the return interval, there is little net effect of wind disturbance (Espírito-Santo et al., 2014; Gloor et al., 2009). Meanwhile, slower recovery rates indicate that windthrows have the potential to create a strong legacy on biomass and functional composition patterns (Chambers et al., 2013; Marra et al., 2014; Negrón-Juárez et al., 2018; Rifai et al., 2016).

Here, we quantified how net biomass change (and its component processes of biomass increment and loss) and functional composition developed with time since disturbance as a function of windthrow severity in Central Amazon forests located near Manaus, Brazil. Windthrow severity was estimated as the fraction of windthrow tree mortality derived from observed change in the fraction of non-photosynthetic vegetation in Landsat pixels for events occurring in 1987, 1996, and 2005. Combining repeated inventories of wind-thrown forests, locally calibrated biomass estimation models, and functional trait data, we empirically modeled the dynamics of biomass and community mean wood density to investigate how the biomass trajectory of forest recovery and its components varied with windthrow severity. We address the following questions: (a) What is the influence of windthrow severity on the recovery of biomass stocks? (b) Which processes (i.e., biomass increment and loss) and associated mechanisms (i.e., tree growth, recruitment, resprouting, and post-windthrow mortality) determine the successional dynamics of net biomass change? (c) What is the role of disturbance-driven species turnover (specifically indicated by community mean wood density and functional composition) in net biomass change and forest resilience?

2 | MATERIALS AND METHODS

2.1 | Study sites and windthrow tree mortality estimations

Study sites are located in the Central Amazon, Brazil (Figure 1a) and are predominantly typical *terra-firme* forest, the most common forest type in the Amazon basin (Braga, 1979). In our study region, forests have dense understory and closed canopy with high tree-species diversity; for example, more than 280 species are reported in a 1-ha plot (de Oliveira & Mori, 1999). The terrain is undulating, with elevation between 40 and 123 m (Supporting Information Table S1). Area-weighted mean elevation for subplots was calculated from a digital elevation model with 30 m × 30 m spatial resolution (Shuttle Radar Topographic Mission, SRTM).

Detailed information on sites, subplots and their selection is provided in Supporting Information Appendix S1. Briefly, we identified windthrows occurring over a 20-year period (1984–2005) using Landsat 5 Thematic Mapper imagery (L5, 30 m × 30 m resolution) (Chambers et al., 2013). Windthrows were identified by their spectral characteristics and distinct shape (Araujo, Nelson, Celes, & Chambers, 2017; Chambers et al., 2007; Nelson et al., 1994). After excluding data with cloud cover, white-sand and floodplain forests, and forests close to human-affected areas (e.g., roads and settlements), we identified sites integrating large-scale single events (i.e., several windthrows created at the same time). Each site was surrounded by old-growth forest and included a large gradient of windthrow tree mortality. Including logistical considerations such as the distance to Manaus and accessibility, we selected three sites with windthrows that occurred in: 2005 (*Site 1*, total windthrown and sampled areas of ~250 ha and 3.6 ha, respectively), 1996 (*Site 2*, ~900 ha, 3 ha), and 1987 (*Site 3*, ~75 ha, 3 ha). We included an additional old-growth forest site (*Site 4*, sampled area of 10 ha) as a large-area control contiguous to *Site 1*. *Site 4* is a well-studied forest (da Silva et al., 2002; Marra et al., 2014) known to have experienced no major natural or human disturbance in the last ~55 years.

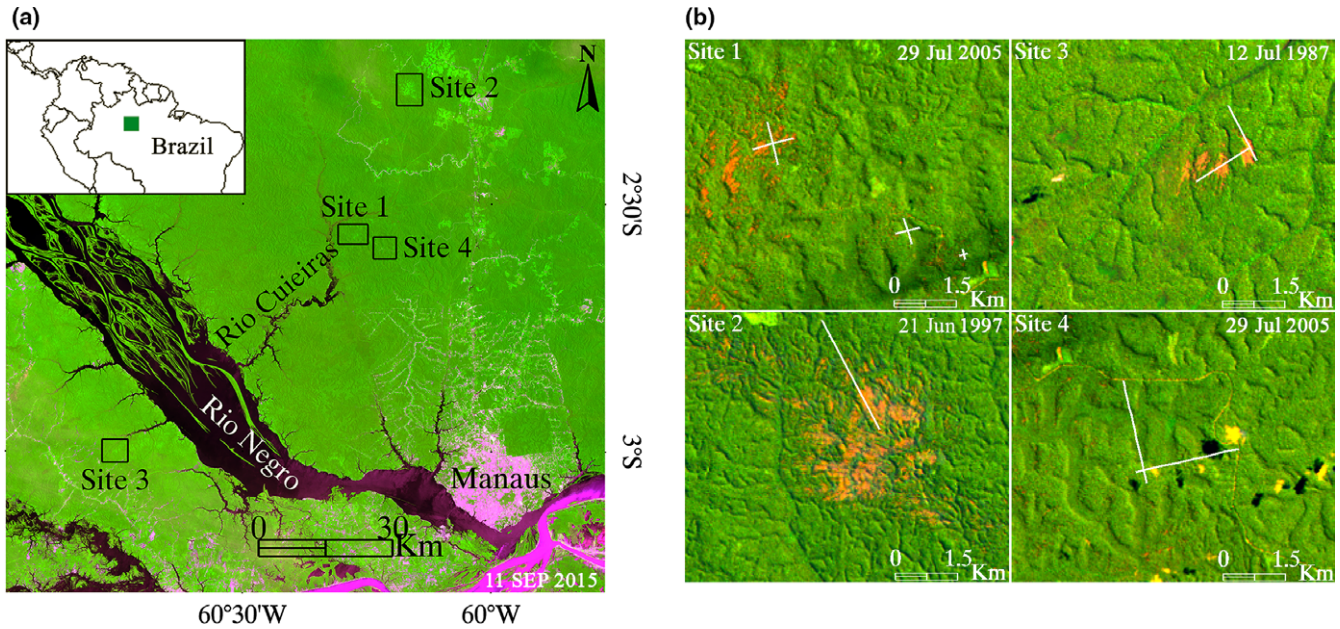

FIGURE 1 Study region: (a) sites comprising chronosequences of Central Amazon forests spanning 4–27 years of recovery from windthrows (*Sites 1–3*) and an old-growth forest (*Site 4*), and (b) transects used to sample the vegetation across the existing tree-mortality gradient (0%–70%). Patches exhibiting high short-wave infrared reflectance (red channel) indicate increases in non-photosynthetic vegetation (NPV) (green channel, near infrared) as a result of the windthrow tree mortality [Colour figure can be viewed at wileyonlinelibrary.com]

We applied spectral mixture analysis (SMA) (Adams & Gillespie, 2006) on selected L5 scenes using methodology applied in previous studies (Chambers et al., 2013; Negrón-Juárez et al., 2010, 2011). SMA allows for the quantification of the per-pixel fraction of the following selected endmembers: green vegetation (GV, i.e., photosynthetic active), dead plant material (NPV, i.e., non-photosynthetic), and shade. The GV and NPV fractions before and after the windthrows were normalized without shade. We used normalized ΔNPV images (i.e., NPV before – NPV after the windthrows) to assess windthrow severity across the selected sites (see Supporting Information Appendix S2 for further details).

Based on SMA and field observations, we defined the position and orientation of transects that crossed major windthrown areas but also included forest patches not affected by the windthrows. Such undisturbed areas were used as references for "pre-disturbance" forest conditions for our response variables. Using transects allowed us to account for the pixel-level variation in windthrow tree-mortality, size, and geometry of gaps (Araujo et al., 2017; Marra et al., 2014; Negrón-Juárez et al., 2011) while keeping fieldwork logistically feasible. Hence, transects include local variation in topography and a wide range in windthrow tree mortality, ranging from undisturbed subplots to subplots with 70% windthrow tree mortality (Magnabosco Marra, 2016; Marra et al., 2014; Negrón-Juárez et al., 2018).

Overall, we monitored forest biomass change and species turnover in 594 subplots nested in transects (also for the old-growth forest in *Site 4*, Supporting Information Appendix S1), with subplots in a given site ranging in size from 250–400 m^2. As in previous studies (dos Santos et al., 2016; Marra et al., 2014), we estimated windthrow severity as the percentage of tree mortality (i.e., trees ≥10 cm diameter at breast height, DBH) at the subplot level by employing a locally parameterized model that has ΔNPV alone as predictor (Negrón-Juárez et al., 2010). We calculated subplot ΔNPV as the area-weighted mean of adjacent pixels. Estimated windthrow tree-mortality ranged from 0%–70%, 0%–57%, and 0%–56% in *Site 1*, *Site 2*, and *Site 3*, respectively (see Supporting Information Table S1 for site-specific details). *Site 4* experienced background tree mortality typical for old-growth forests in the region, that is, ~2% per year (da Silva et al., 2002; Toledo, Magnusson, Castilho, & Nascimento, 2011).

2.2 | Forest monitoring and biomass estimation

In each subplot, we tagged and measured the DBH of all trees ≥10 cm DBH. We inventoried each site at least twice between 2002 and 2016 (always in the dry season), which in total amounted to more than 13,000 trees being monitored. Repeated inventories of the sites in our chronosequence allowed us to test patterns of biomass recovery and dynamics with and without the need to substitute space for time. *Site 4* has been monitored since 1996, with consecutive inventories every two to three years. For this site, we used data from the years 2002 and 2004, for which we had species identification at high resolution and imagery data confirming that within this time period this forest experienced no detectable windthrows. Within each study site, we collected botanical samples from at least one individual of all recorded species (Supporting Information Appendix S3). When possible, identification was carried out to the species level.

We assessed dry aboveground biomass in our chronosequences using a biomass estimation model calibrated with 727 locally harvested trees that have DBH and species' functional group as predictors (Magnabosco Marra et al., 2016). To check for the consistency of our results, we estimated biomass using two other models using either DBH and wood density or DBH alone as predictors. We calculated dry aboveground biomass stocks for subplots by summing up the biomass of individual trees. Wood density data were compiled from studies carried in the Amazon (Chave et al., 2009; Fearnside, 1997; Laurance et al., 2006; Magnabosco Marra et al., 2016; Nogueira, Fearnside, Nelson, & França, 2007; Nogueira, Nelson, & Fearnside, 2005). Trees were assigned to one of three functional groups (pioneer, mid- and late-successional) describing the main differences in each species' life history, architecture, and traits (Supporting Information Appendix S3) (Magnabosco Marra et al., 2016).

2.3 | Data analysis

It was necessary to use small subplots for their size to be approximately the same as the smallest size class of windthrows in our study. On the other hand, these subplots are too small to average out background spatial heterogeneity in forest structure and floristic composition. For example, the chance inclusion of a single large dense-wooded tree in a small plot creates an unrealistically high stand-level biomass estimate (Clark & Clark, 2000; de Oliveira, Higuchi, Celes, & Higuchi, 2014; Magnabosco Marra et al., 2016). To yield representative and stable estimates of biomass while still allowing for sufficient granularity in a detailed assessment of windthrow tree mortality, we randomly grouped subplots into bins of four (*Site 1*), three (*Site 2–4*), and two (*Site 4*) subplots. These bins (i.e., binned subplots) yielded approximately similar total areas of 1,200 m^2, 900 $m^{2,}$ and 800 m^2, respectively (Supporting Information Appendix S4).

We did not detect consistent differences in biomass stocks across the existing elevational gradient in *Site 4* (i.e., 61–123 m), which suggests that topography does not shape biomass patterns in our study region (linear model, df = 122, F = 2.2, r^2_{adj} = 0.009, and p = 0.141). Moreover, windthrows were observed in all the topographic classes and elevation ranges included in our study sites. Therefore, we binned subplots from *Sites 1–3* using windthrow tree-mortality as a single grouping variable. For *Site 4*, we binned subplots randomly. We calculated windthrow tree mortality and elevation for bins as the mean of corresponding subplot values. Further analyses were conducted on mean values of bins.

We used the data from *undisturbed bins* (hereafter referred to as the undisturbed chronosequence) to assess relative biomass recovery and changes in community mean wood density (abundance weighted, Supporting Information Appendix S5) in the *windthrown*

bins (hereafter referred to as the *windthrow chronosequences*). With that, we aimed at accounting for possible pre-disturbance differences on biomass stocks and community mean wood density among sites.

To define the undisturbed chronosequence, we applied a threshold of windthrow tree mortality ≤4%. This number reflects the maximum background tree-mortality rates (Lugo & Scatena, 1996) reported for local-regional old-growth forests not affected by large-scale windthrows (Johnson et al., 2016; Marra et al., 2014; Toledo et al., 2011). We defined the severity of windthrow chronosequences based on estimates of windthrow tree mortality: *low*- 4%–20% (12% and 19%, mean and maximum, respectively); *moderate*-20%–40% (29% and 39%); and *high*- >40% (49% and 65%).

We monitored four mechanisms of biomass increment (i.e., regrowth) and two of biomass loss (i.e., post-windthrow mortality). Mechanisms of biomass increment include: diameter growth of survivor trees (includes those recruited after the windthrows but with DBH ≥10 cm in our first inventories), diameter growth from recruits (i.e., trees that were recruited in our second inventories and followed in a subsequent inventory), diameter growth from resprouters with mechanical injuries likely to have been caused by the respective windthrows (i.e., snapped, uprooted, and crown-injured trees), and recruitment (trees crossing our 10 cm DBH threshold). Although resprouting does not include direct measures of biomass increment resulting from changes in crown area and/or volume (i.e., regrowth of branches or leaves), the trunk accounts for ~65% of the total biomass of trees in our study region (Higuchi, Santos, Ribeiro, Minette, & Biot, 1998). Growth from recruits was only measured for *Site 1* (7–10 years since disturbance) and *Site 2* (17–20 years since disturbance), for which we had three consecutive forest inventories. Mechanisms of biomass loss include post-windthrow mortality of undamaged trees and those that suffered trunk and/or crown damage (i.e., resprouters). Net biomass change was calculated as biomass increment minus biomass loss for the time period between forest inventories.

In repeated forest inventories, assumptions about the prior biomass of recruits crossing the 10 cm DBH threshold will affect overall biomass estimates. For instance, assuming that recruits had zero initial biomass can overestimate the contribution of recruitment to overall biomass increment and net change (Talbot et al., 2014). Therefore, we predicted the DBH of recruits backward by using random forest regression algorithms (Breiman, 2001; Cutler et al., 2007) and calculated the biomass increment as the difference between the predicted and the measured DBH (see details in Supporting Information Appendix S5). As an alternative to using community mean values (Talbot et al., 2014), this approach allowed us to reliably account for species differences in growth due to the heterogeneous and dynamic environmental conditions of windthrows. Still, our predictive models of annual growth (both calibration and validation) tended to underestimate observable valuables (Supporting Information Table S2 and Figure S2).

We fitted *generalized additive models* (GAMs) to capture non-linear relationships of biomass change and its components to our main predictors, time since disturbance and windthrow tree mortality. GAMs can include multiple non-parametric smoothing functions, which do not require an a priori assumption of the functional form between the response and predictor variables, and can fit models with different error distributions (Hastie & Tibshirani, 1990; Wood, 2006) (Supporting Information Appendix S6). We used the two predictors (and their interaction) as fixed smooth-terms. Although elevation was not an important variable driving biomass stocks in our old-growth forests, there is evidence that windthrow damage and tree-mortality are mediated by topography (Goulamoussène, Bedeau, Descroix, Linguet, & Hérault, 2017; Marra et al., 2014; Rifai et al., 2016). To account for that, we considered the interaction between windthrow tree mortality and elevation as an additional fixed smooth-term. Due to site differences in range and mean values of elevation, we included the interaction between this variable and sites as a random smooth-term. We used the total area of bins as observation weights during model fitting (Nelder & Wedderburn, 1972; Wood, 2006).

For graphical display, we predicted net biomass change and its components as a function of time since disturbance for four levels of windthrow tree mortality: 4%, 20%, 40%, and 65%. These values span the range of windthrow tree mortality observed in our study sites (i.e., after binning). We checked the precision of our estimates by calculating 95% confidence intervals using standard errors from predictions (Supporting Information Appendix S6).

To check for possible biases on model results due to our binning approach, we fit equivalent GAMs with non-binned (i.e. subplot-level) data for all investigated processes (Supporting Information Figure S3 and Table S3). Here, we tested for spatial autocorrelation of subplots along the transects by fitting an extra model in which subplots was included as an additional random smooth-term (Wood, 2006). The models fit with subplot-level data showed similar patterns but had, as expected, lower explanatory power than those fit with binned data (Supporting Information Table S4). Spatial autocorrelation for subplots on estimates of relative biomass stocks and community mean wood density was minor and including this term did not change model residuals substantially. This indicated that the effects of subplots nested in transects were negligible.

3 | RESULTS

3.1 | Impacts of windthrows on biomass stocks

Although we observed continuous biomass recovery over time (i.e., trees ≥10 cm DBH, 4–27 years since disturbance), windthrows produced reductions in biomass stocks that persisted for decades (Figure 2a and Supporting Information Figure S5). The undisturbed chronosequence (i.e., windthrow tree mortality ≤4%) showed no substantial changes in biomass stocks (Figure 2a, dark-blue points).

Four years after disturbance (*Site 1*), mean (± 95% CI) biomass stock in areas experiencing moderate windthrow severity (20%–40% windthrow tree mortality) were 179.4 ± 58.3 Mg/ha while those experiencing high windthrow severity (>40% mortality) were 118 ± 84.3 Mg/ha. These correspond to 64% and 42%, respectively,

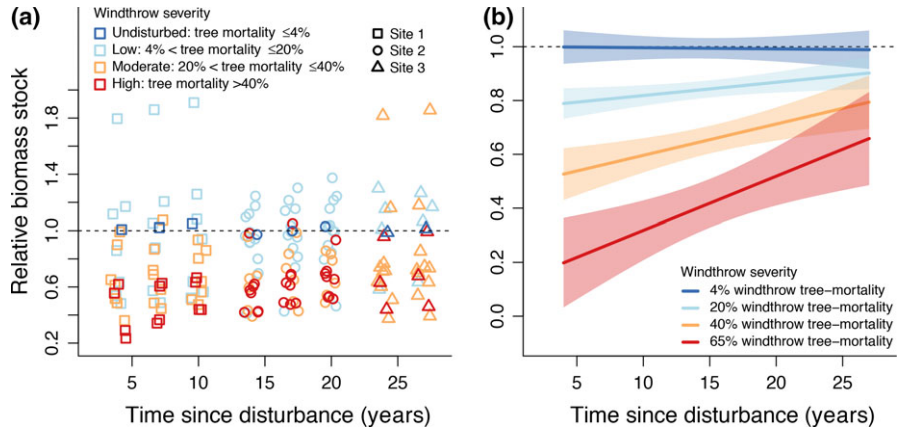

FIGURE 2 Biomass recovery in wind-disturbed forests in Central Amazon, Brazil: (a) relative biomass stocks (i.e., compared to the mean biomass stocks of undisturbed forest patches in the same time period, dark-blue points) and (b) predictions of biomass recovery over time since disturbance for different windthrow severities. In panel *a*, we jittered data points to reduce overlap. Predictions were made with *generalized additive models* (GAMs) fit with time since disturbance and windthrow tree mortality (and their interaction) as predictors (see Supporting Information Table S4 for details). Shaded areas indicate the 95% confidence intervals of predictions. Data on biomass stocks are summarized in Supporting Information Figure S5. See Supporting Information Figure S3 for results using non-binned data [Colour figure can be viewed at wileyonlinelibrary.com]

of the biomass in the undisturbed forest at *Site 1* (279.9 ± 40.5 Mg/ha) (Figure 2a and Supporting Information Figure S5). After 27 years (Site 3), biomass stocks had not yet fully recovered and had reached 82% (moderate severity; 195.2 ± 69 Mg/ha) and 70% (high severity; 165.9 ± 155.4 Mg/ha) of the undisturbed forest in *Site 3* (237.3 ± 41.1 Mg/ha). Across all sites, the areas experiencing low windthrow severity (4%–20% windthrow tree mortality) had large variation of biomass stocks—from 48% (133.9 Mg/ha) to 191% (530 Mg/ha) of those observed in the undisturbed chronosequence. High biomass in windthrow chronosequences reflects single subplots with higher-than-average numbers of large trees (i.e., DBH between 50–134 cm) that contributed to very high estimates of biomass stocks (e.g. 1,389.3 Mg/ha and 1,058.6 Mg/ha in *Site 1* and *Site 3*, respectively).

We tested the effect of a number of model approaches and assumptions on predictions of biomass recovery and its components. Elevation and its interaction with windthrow tree mortality had only a marginal effect on biomass recovery for non-binned and binned data (Supporting Information Tables S3 and S4, respectively). However, variations in elevation were also not independent from sites and accounting for this variable did not increase the model's explanatory power substantially.

Tree density varied strongly across our studied sites—27, 54 and, 91 trees per bin (minimum, mean and maximum, respectively). Still, our model fit with only time since disturbance and windthrow tree mortality explained 41.8% (adjusted coefficient of determination, r^2_{adj} = 0.39) of the variation in biomass stocks in our study sites (Figure 2b and Supporting Information Figure S4a). Relative biomass recovery and measures of fit for non-binned data are given in Supporting Information Figure S3 and Table S3, respectively.

Windthrow tree mortality influenced not only biomass stocks, but also recovery rates. The predicted time to recover "pre-disturbance" biomass (i.e., at least 90% of reference stocks) for areas experiencing 20%, 40%, and 65% windthrow tree mortality were 27 years, 37 years and, 40 years, respectively (Table 1 and Supporting Information Table S5). Low windthrow severity resulted in substantial reductions of biomass stock, and the predicted recovery rate over 4–27 years was lower (0.49% per year, ~1.3 Mg ha^{-1} year^{-1}, all sites) than that for moderate (1.16% per year, ~3 Mg ha^{-1} year^{-1}) and high (2% per year, ~5.1 Mg ha^{-1} year^{-1}) windthrow severity. Overall patterns of biomass were similar, but recovery was faster when using two other allometric models for estimating tree biomass. Including predictors that account for allometric differences among species requires a longer time to recover (Supporting Information Table S5).

3.2 | Rates and mechanisms of biomass change

While biomass increment due to standing tree growth was relatively constant over time in undisturbed chronosequence (~3.5 Mg ha^{-1} year^{-1}, all sites), in windthrow chronosequences it varied substantially (from 2.1 Mg ha^{-1} year^{-1} to 7.6 Mg ha^{-1} year^{-1}). Overall, biomass increment in windthrow chronosequences increased at rates (from 3.9 ± 0.4 Mg ha^{-1} year^{-1} to 6.3 ± 1.4 Mg ha^{-1} year^{-1}) that persisted for more than 15 years (Figure 3a and Supporting Information Figure S6).

Rates of biomass loss in windthrow chronosequences were more variable (i.e., from no loss to −26.9 Mg ha^{-1} year^{-1}) compared to undisturbed forest patches (from −1.3 Mg ha^{-1} year^{-1} to −3.1 Mg ha^{-1} year^{-1}), and indicated continued mortality of survivor trees during the decades following disturbance (Figure 3c and Supporting Information Figure S6). Although uncertainties are large, mean rates of biomass loss in windthrow chronosequences (ranged from −0.7 ± 0.3 Mg ha^{-1} year^{-1} to −7.5 ± 8.7 Mg ha^{-1} year^{-1}) were up to 3.4-fold higher than rates in the undisturbed chronosequence (~−2.2 Mg ha^{-1} year^{-1}, all sites). Overall, post-windthrow mortality

TABLE 1 Predictions (mean ± 95% confidence intervals) of biomass patterns and relative wood density in wind-disturbed forests in Central Amazon, Brazil. Predictions were made with *generalized additive models* (GAMs) fit with time since disturbance and windthrow tree mortality (and their interaction) as predictors. See Supporting Information Figure S4 and Table S4 for details

Time since disturbance (years)	Windthrow tree-mortality (%)	Relative biomass stock (Mg ha^{-1} year^{-1})	Biomass increment (Mg ha^{-1} year^{-1})	Biomass loss (Mg ha^{-1} year^{-1})	Net biomass change (Mg ha^{-1} year^{-1})	Relative wood density
4 and 5.5	4	0.998 ± 0.062	3.493 ± 0.311	−2.85 ± 1.118	0.629 ± 1.111	1 ± 0.01
15 and 15.5	4	0.994 ± 0.038	3.781 ± 0.217	−2.401 ± 0.7831	1.374 ± 0.777	0.97 ± 0.01
27 and 25.5	4	0.988 ± 0.071	4.07 ± 0.396	−1.947 ± 1.422	2.119 ± 1.413	0.99 ± 0.01
4 and 5.5	20	0.788 ± 0.056	4.203 ± 0.29	−3.791 ± 1.26	0.484 ± 1.235	0.99 ± 0.02
15 and 15.5	20	0.843 ± 0.031	4.211 ± 0.225	−3.2 ± 0.925	1.043 ± 0.9	0.93 ± 0.01
27 and 25.5	20	0.902 ± 0.06	4.218 ± 0.394	−2.61 ± 1.322	1.603 ± 1.302	0.91 ± 0.02
4 and 5.5	40	0.526 ± 0.096	5.051 ± 0.484	−3.83 ± 1.774	1.254 ± 1.759	0.95 ± 0.02
15 and 15.5	40	0.654 ± 0.051	4.634 ± 0.285	−3.068 ± 1.039	1.581 ± 1.03	0.88 ± 0.01
27 and 25.5	40	0.793 ± 0.098	4.217 ± 0.536	−2.307 ± 1.92	1.907 ± 1.908	0.86 ± 0.02
4 and 5.5	65	0.198 ± 0.165	6.058 ± 0.837	−2.374 ± 3.53	3.48 ± 3.468	0.87 ± 0.04
15 and 15.5	65	0.418 ± 0.089	5.011 ± 0.698	−1.399 ± 2.831	3.516 ± 2.746	0.84 ± 0.03
27 and 25.5	65	0.658 ± 0.173	3.964 ± 1.286	−0.423 ± 4.203	3.553 ± 4.118	0.85 ± 0.06

Note. Time since disturbance is given for relative biomass stock and wood density, and net biomass change (and its components), respectively.

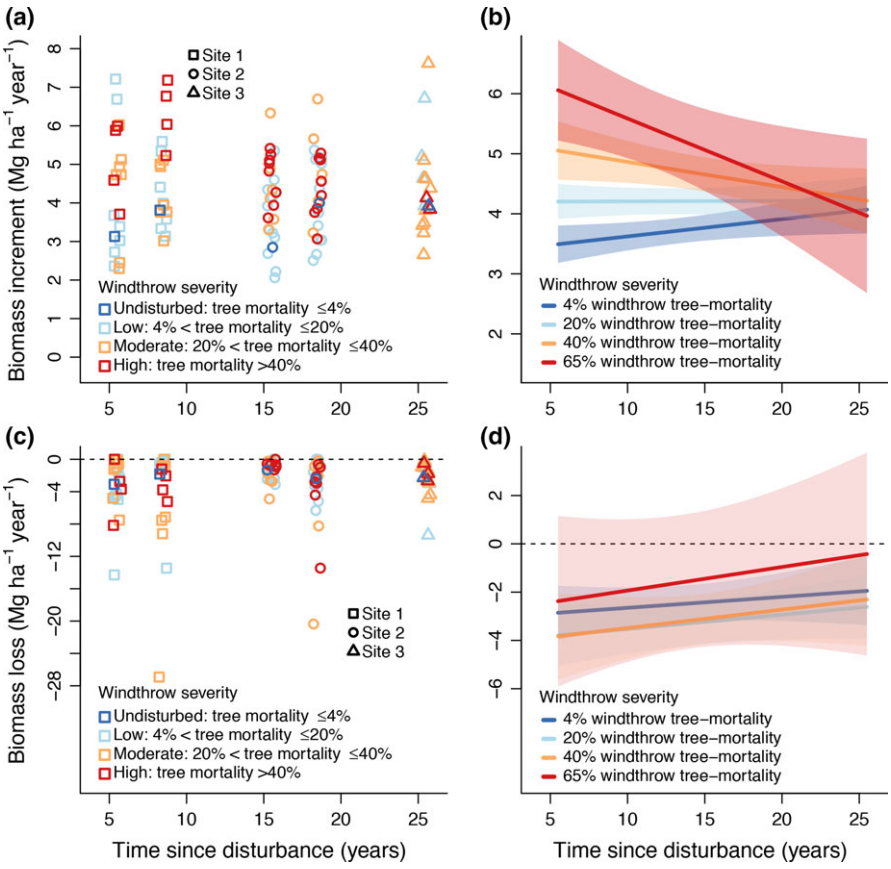

FIGURE 3 Biomass balance in wind-disturbed forests in Central Amazon, Brazil: observed (a and c) and predicted (b and d) biomass increment (i.e., tree growth plus recruitment) and loss (i.e., post windthrow tree mortality) over time since disturbance for different windthrow severities. In panels a and c, we jittered data points to reduce overlap. Dark-blue points are mean values in undisturbed chronosequences. Predictions were made with *generalized additive models* (GAMs) fit with time since disturbance and windthrow tree mortality (and their interaction) as predictors (see Supporting Information Table S4 for details). Shaded areas indicate the 95% confidence intervals of predictions. Data on biomass increment and loss are summarized in Supporting Information Figure S6 [Colour figure can be viewed at wileyonlinelibrary.com]

losses were lowest at high windthrow severity (~−2.5 Mg ha^{-1} year^{-1}, all sites) and highest at low (~−2.8 Mg ha^{-1} year^{-1}) and moderate (~−3.8 Mg ha^{-1} year^{-1}) windthrow severities.

Our GAM model based on time since disturbance and windthrow tree mortality explained 25.9% (r^2_{adj} = 0.21) of the variation in biomass increment (Supporting Information Figure S4b and Table S4). Including elevation resulted in similar predicted biomass recovery and its inclusion in our model increased explanatory power by 4%. Predicted rates of biomass increment in the windthrow chronosequences declined systematically with time since disturbance but remained largely different from those of the undisturbed chronosequence for more than two decades (Figure 3b and Table 1).

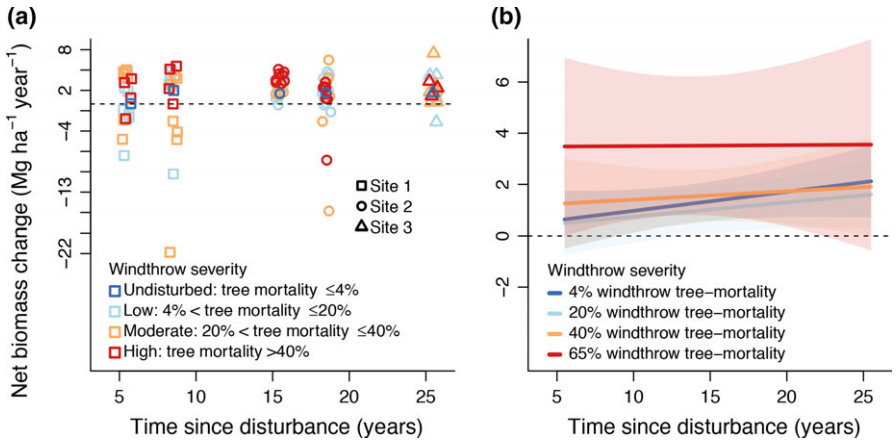

FIGURE 4 Net biomass change (i.e., biomass increment minus loss) in wind-disturbed forests in Central Amazon, Brazil: (a) observed and (b) predicted net biomass change over time since disturbance for different windthrow severities. In panel *a*, we jittered data points to reduce overlap. Dark-blue points are mean values of biomass net change in undisturbed forest patches. Predictions were made with *generalized additive models* (GAMs) fit with time since disturbance and windthrow tree mortality (and their interaction) as predictors (see Supporting Information Table S4 for details). Shaded areas indicate the 95% confidence intervals of predictions [Colour figure can be viewed at wileyonlinelibrary.com]

By contrast, our model captured only 4.5% (r^2_{adj} = 0.01) of the overall variation in biomass loss, indicating weak control of immediate windthrow tree mortality (Supporting Information Figure S4c and Supporting Information Table S4). Biomass loss tends to decrease over time for any given chronosequence (Figure 3c and d and Table 1). Our model suggests that post-windthrow biomass losses tend to be highest at moderate windthrow severity. This indicates a delayed negative effect of windthrows on the carbon balance. Elevation and its interaction with sites had only a marginal effect on observable patterns of biomass loss and did not increase model explanatory power.

Biomass accumulated in the undisturbed chronosequence at relatively consistent rates of ~1.4 Mg ha^{-1} year^{-1} (Figure 4a). In windthrow chronosequences, the altered rates of biomass increment and loss drove large variations in rates of net biomass change (i.e., from −21.8 to 7.5 Mg ha^{-1} year^{-1}). Although some disturbed areas lost biomass (i.e., biomass increment smaller than loss), windthrow chronosequences showed an overall net increase in biomass at rates up to two times higher (4 ± 0.7 Mg ha^{-1} year^{-1}) than in the undisturbed chronosequence (maximum of 2 ± 1.3 Mg ha^{-1} year^{-1}).

The large uncertainties associated with our predictions of biomass loss dominated the uncertainties in predictions of net biomass change. Thus, GAMs based on time since disturbance and windthrow tree mortality explained only 5% (r^2_{adj} = 0.02) of the observed variation in net biomass change. Elevation and its interaction with windthrow tree mortality and sites did not affect predictions of net biomass change (Supporting Information Figure S4d and Table S4).

While the net biomass change following high windthrow severity was mainly driven by rapid growth coupled with low rates of mortality, the smaller rates of net biomass change observed after low and moderate windthrow severity mostly reflected an increased and variable post-windthrow mortality of trees. Although with a high associated uncertainty (Figure 4b), predicted net biomass change in the windthrow chronosequences was up to 1.7 times (3.5 ± 4.1 Mg ha^{-1} year^{-1}) that observed in the old-growth forest used as a control (2.1 ± 1 Mg ha^{-1} year^{-1}). Note that biomass increment and loss only account for live biomass—that is, we did not quantify decomposition of coarse woody debris on the forest floor.

The importance of different mechanisms of biomass increment and loss was strongly influenced by windthrow severity (Figure 5). Growth of survivor trees (as opposed to different forms of recruitment) accounted for 99.8% and ~95% of the observed biomass increment in *Site 4* and in the undisturbed chronosequence (all sites). In contrast, recruitment and subsequent growth of those recruits increased in importance with windthrow severity, especially during the initial years of recovery. Together they accounted for up to 23.5% (5.5 years, only recruitment) and 49.1% (8.5 year, recruitment plus growth of recruits) of the total biomass increment at *Site 1*. The increased importance of these mechanisms resulted in shifts of the size distribution in these forests toward smaller trees (Supporting Information Figure S7). The contribution of resprouting trees to biomass recovery was generally low but was of higher importance in moderate and high windthrow severity and toward later phases of recovery (15.5 years, 18.5 years and 25.5 years), contributing a maximum of 11% (15.5 years) of the total biomass increment.

Post-windthrow mortality of damaged trees accounted for up to 23% (8.5 years) of the overall biomass loss post-windthrow, with largest losses at low to moderate windthrow severities. Within sites, the losses occurred during different inventory periods, for example, at low severity after 5.5 years and at moderate severity only after 8.5 years. Elevated post-mortality losses were still noticeable at low to moderate windthrow severity after 15.5 years (moderate), 18.5 years (moderate), and 25.5 years (low).

3.3 | Species turnover and wood density

Site 4 and the undisturbed chronosequence were dominated by late-successional species with a community mean wood density of

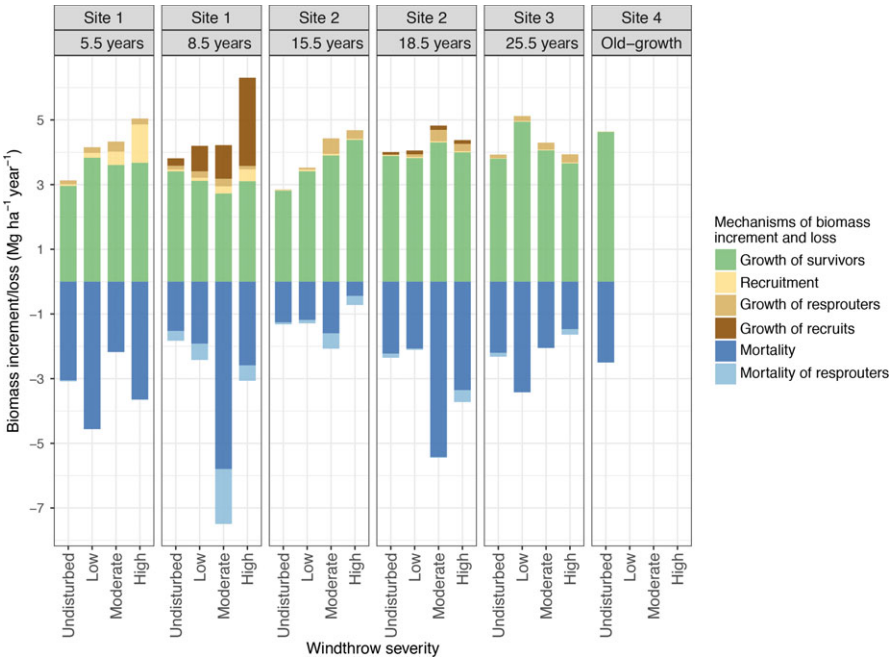

FIGURE 5 Mechanisms of biomass increment and loss in *terra-firme* forests of the Central Amazon, Brazil. The data set includes an old-growth forest (*Site 4*) used as a control and three sites (*Sites 1–3*) that experienced a wide gradient of windthrow tree mortality (up to 70%) and that span 4–27 years of recovery (see Figure 1 and Supporting Information Table S1 for details). Windthrow severity: Undisturbed windthrow tree-mortality ≤4%; Low- 4%–20%; Moderate- 20%–40%; High- >40%. Mechanisms: Survivors- biomass increment by survivor trees (includes those recruited after the windthrows but with DBH ≥10 cm in our first inventories); Recruitment- biomass increment by trees crossing our 10 cm DBH threshold; Resprouting- biomass increment by trees with damage/injuries in the trunk and/or crown; Recruits- biomass increment by trees that were recruited in our second forest inventory and followed in a subsequent inventory; Mortality- biomass loss by dead trees; Mortality of resprouters- biomass loss by dead trees with damage/injuries in the trunk and/or crown [Colour figure can be viewed at wileyonlinelibrary.com]

0.703 ± 0.004 g/cm^3 and ~0.704 g/cm^3 (all sites), respectively (Figure 6a and Supporting Information Figure S8). In contrast, windthrows produced strong and persistent reductions in community mean wood density (minimum of 0.551 g/cm^3) and changed the biomass partitioning among functional groups, that is, pioneers versus mid- versus late-successional species (Supporting Information Figure S9) over the 4–27 years of recovery we studied.

Our model including time since disturbance and windthrow tree mortality captured 68% (r^2_{adj} = 0.64) of the overall variation of relative wood density in our windthrow chronosequences (Figure 6b and Supporting Information Figure S4e and Supporting Information Table S4). Elevation had no effects on variations of community mean wood density.

4 | DISCUSSION

Both time since disturbance and windthrow severity were important factors explaining the 8.1-fold variation in biomass stocks across different sites in the Central Amazon. Windthrow severity controls the trajectory of forest recovery in several ways. The severity of the windthrow event determines the initial reduction in biomass. The size of the gaps created and the increased light availability and nutrients released from necromass in turn impacts the trajectory of subsequent processes. In the initial phase of recovery (5.5 years since disturbance), recruitment was a major biomass recovery mechanism in areas suffering high windthrow severity, while growth by surviving trees was more important for areas experiencing low and moderate severity windthrow. At later stages (8.5–25.5 years), growth by recruits and especially resprouted trees remained important but new recruitment ceased quickly. Post-windthrow biomass losses, though hard to predict, were generally substantial even over almost two decades after the windthrow events. Even though biomass recovered up to 70%–82% of pre-disturbance values over the ~25 years in our oldest chronosequence site, changes in the relative dominance of functional groups from late successional (undisturbed) to mid successional and pioneer species (disturbed) indicate long-lasting effects of windthrows manifested in less dense wood that is also less resistant to new disturbances. Our results suggest that windthrows have the potential to create a functional and taxonomic legacy affecting the biomass/carbon balance at the landscape level in Amazon *terra-firme* forests.

4.1 | Biomass patterns along recovery

We observed high rates of windthrow tree mortality and damage. These are consistent with high wind speeds reported for the Amazon (e.g. 68–147 km/hr; Negrón-Juárez et al., 2018; Garstang et al., 1998) that have been hypothesized to cause widespread tree mortality. This finding demonstrates that Amazon downbursts have destructive power similar to that of other tropical storms (Burslem

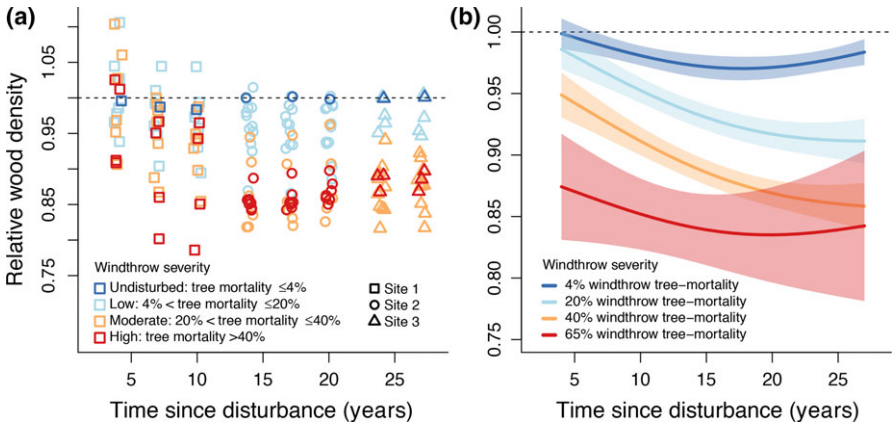

FIGURE 6 Effects of windthrows on community mean wood density in Central Amazon forests, Brazil: (a) observed relative wood density (i.e., compared to the mean wood density of undisturbed forest patches in the same time period, dark-blue points) and (b) predicted changes in relative wood density over time since disturbance for different windthrow severities. In panel a, we jittered data points to reduce overlap. Predictions were made with *generalized additive models* (GAMs) fit with time since disturbance and windthrow tree mortality (and their interaction) as predictors (see Supporting Information Table S4 for details). Shaded areas indicate the 95% confidence intervals of predictions. Data on wood density are summarized in Supporting Information Figure S7 [Colour figure can be viewed at wileyonlinelibrary.com]

et al., 2000; Everham & Brokaw, 1996; Hjerpe, Hedenâs, & Elmqvist, 2001; Mascaro et al., 2005; Scalley et al., 2010; Scatena, Moya, Estrada, & Chinea, 1996).

High rates of windthrow tree mortality are predicted to induce equally high rates of biomass recovery. Yet, biomass recovery rates in our study sites were comparably slower than in a forest in Puerto Rico that experienced 50% loss of biomass in a hurricane. In this forest, net biomass change during the first 5 years (16.3 Mg ha^{-1} year^{-1}; Scatena et al., 1996) and over a 15-year period (8 Mg ha^{-1} year^{-1}; Scalley et al., 2010) were 4.5- and 2.2-fold higher (respectively) than the maximum predicted value in our windthrow chronosequences (3.6 Mg ha^{-1} year^{-1}). Hurricane-damaged forests in Nicaragua experiencing a 73% biomass loss had recovered ~34% of initial values over a 11-year period of recovery and net biomass change averaged 5.4 Mg ha^{-1} year^{-1} (Mascaro et al., 2005).

While our biomass recovery rates were lower than in these Central American forests—most likely due to differences in forest structure and environmental conditions—they were substantially higher than recovery rates found after selective logging. Forests recovering for a similar time period (i.e., 1–33 years) following a 10%–50% biomass loss due to logging had predicted recovery times ranging from 12 to 75 years (Rutishauser et al., 2015) as opposed to a maximum of 40 years required to recover the biomass lost after 65% tree-mortality in our windthrown sites. There are several potential causes for the apparently faster biomass recovery in windthrows. In contrast to most human disturbances, windthrows do not alter the seed and seedling/sapling banks and retain nutrients via the incorporation of recalcitrant fractions of necromass into the soil (dos Santos et al., 2016; Vitousek & Denslow, 1986). Furthermore, windthrows, unlike logging, have a complex geometry (Araujo et al., 2017; Marra et al., 2014; Nelson et al., 1994). A higher perimeter per area of disturbed forest creates a more effective interface with adjacent undisturbed forest patches acting as seed sources. In addition, windthrows provide particular niches, such as pits and mounds of uprooted trees (Putz, 1983), where several species can germinate and establish (Marra et al., 2014; Ribeiro et al., 2014).

Biomass loss reported for an Amazon forest recovering from logging for a 4-year period was 1.6-fold higher (Mazzei et al., 2010) than the maximum value we observed in a similar period of recovery from windthrows (–4.6 Mg ha^{-1} year^{-1}, 5.5 years). Higher recovery rates and lower loss rates suggest that these forests have a higher resilience to windthrow than to logging. Biomass loss due to post-windthrow mortality was predominantly stochastic and may have a range of causes such as delayed mortality of damaged/disease-prone trees, competition with newly incoming regeneration, physiological stress after exposure to altered environmental conditions, and increased susceptibility to recurrent smaller scale wind disturbances (Laurance & Curran, 2008; Laurance et al., 2006; Schwartz et al., 2017). We showed that delayed mortality is particularly important in windthrows with low to moderate severity. Our data suggest that care should be taken when estimating mortality from satellite images that only capture the signal of the initial mortality wave but miss such delayed mortality. Furthermore, modeling post-windthrow carbon loss will require more information on the fate of the necromass produced during windthrows (dos Santos et al., 2016), which was not included in this study.

4.2 | Wind-induced changes in vital rates, functional composition, and community wood density

Biomass increment in our old-growth forest and undisturbed chronosequence was dominated by growth of adult trees. In contrast, biomass increment in windthrows was largely driven by additional recruitment (i.e., trees crossing the 10 cm DBH threshold), which has also been observed in other tropical forests recovering from storms (Burslem et al., 2000; Hjerpe et al., 2001; Vandermeer

et al., 2000). In our sites, the threshold for predicting when this mechanism of recovery begins to dominate occurs when windthrow tree mortality exceeds 20% (i.e., ~10 of the ~54 dead trees in a single Landsat pixel) (Chambers et al., 2013; Negrón-Juárez et al., 2018). Interestingly, despite significant rates of post-windthrow mortality, the growth of *survivor trees* was equal to or greater than the tree growth in the undisturbed control sites already during early recovery phase (5.5 years). There are two possible causes for this: (a) an increase in growth rates of survivors released from competition compensate for the wind-induced loss of individuals; or (b) recruitment and the activation of the sapling bank happens so fast, that many individuals have passed the 10 cm DBH threshold already before the first inventory. We suspect that the former is the main reason for high rates of growth at low to moderate severity, while the latter is the main cause for the even higher growth rates at high severity.

Although many of the species are able to resprout (Marra et al., 2014; Putz & Brokaw, 1989), this mechanism of biomass increment was relatively unimportant. It contributed <11% percent to the overall increment and was observed mostly during later stages of the 4- to 27-year period covered by our study. Importantly, some species may reduce or stop lateral growth to allocate resources to repair/replace crown damage. This allocation of resources to repair crowns may limit DBH growth (Bellingham, Tanner, & Healey, 1994; Mascaro et al., 2005; Yih, Boucher, Vandermeer, & Zamora, 1991), but would not have been identified as *resprouting* in our study.

Although biomass stocks can be completely recovered in the 27–40 years following windthrow, the accumulated biomass is largely in pioneer and mid-successional species with short life spans and low wood density (Chazdon, 2014; Laurance et al., 2004; Swaine & Whitmore, 1988). In our windthrown subplots genera like *Cecropia*, *Conceveiba*, *Guatteria*, *Inga*, *Miconia*, *Pourouma*, *Tachigali*, and *Tapirira* were common. Some of these genera are classically reported to dominate early succession also following general human disturbances (Jakovac, Peña-Claros, Kuyper, & Bongers, 2015; Laurance et al., 2006; Mesquita, Massoca, Jakovac, Bentos, & Williamson, 2015). Thus, the recovery of the functional composition typical for old-growth forests dominated by species with high wood densities (Fauset et al., 2015) is likely to take much longer than four decades.

The successional trajectory of disturbed forests beyond the ~30-year limit imposed by the availability of historical Landsat images (Chambers et al., 2013; Espírito-Santo et al., 2010; Negrón-Juárez et al., 2018) may take different pathways. Studies of forest dynamics after human disturbances (e.g., forest clearing) showed that cohorts of pioneer and mid-successional species may die in synchronized waves once they have reached their maximum longevity. If this is true for succession after windthrow, we might expect net biomass losses over the next several decades (Chazdon, 2014; Mesquita et al., 2015). Alternatively, as observed after logging (Mazzei et al., 2010; Rutishauser et al., 2015), increased abundance and biomass increment in mid- and late-successional species can compensate for such losses and prevent these forests from entering a period of negative net biomass change.

Altered functional composition can imply changes in forest attributes related to its capacity for biomass storage, including the wood physiology and protection, maximum attainable sizes, and crown architecture (Magnabosco Marra et al., 2016; Nascimento & Laurance, 2004; Vieira et al., 2004). For instance, reduced wood density and shorter life spans of early successional cohorts of species (Laurance et al., 2004; Mesquita et al., 2015; Swaine & Whitmore, 1988) can reduce the residence time of woody biomass and accelerate dead wood decay rates (Chambers et al., 2000; Galbraith et al., 2013; Hérault et al., 2010). Most pioneers do not attain tall stature (King, 1996; Magnabosco Marra et al., 2016; Swaine & Whitmore, 1988). Unless they are replaced by late-successional species over the course of succession, the total ecosystem volume captured by the forest remains low, as do carbon stocks. Importantly, forests with smaller and lower wood density pioneer trees can have slower rates of biomass accumulation (Hérault & Piponiot, 2018) and be more vulnerable to new windthrows (Ribeiro et al., 2016; Rifai et al., 2016) and other disturbances such as pathogen attack, drought, fire, and land use/fragmentation (Hérault & Piponiot, 2018; Laurance & Curran, 2008; Schwartz et al., 2017; Silvério et al., accepted).

4.3 | Landscape control and potential implications

Models predicting biomass change following windthrow were not very sensitive to the inclusion of landscape features such as elevation (e.g., variations between plateau and valley conditions). We can therefore conclude that the relationships in our models can be generally applied to Central Amazonian forests irrespective of the topographic position. This finding confirms studies that have shown a weak effect of topographic aspects on the biomass dynamics of old-growth forests (Castilho, Magnusson, Araújo, & Luizão, 2010) and on the recovery trajectory of secondary forests (Hérault & Piponiot, 2018). Additional work in the study region showed that the susceptibility to snapping and uprooting is apparently similar for trees established in upper plateaus and lower valleys (Ribeiro et al., 2016). It is however known that topography controls wind speed and thus the occurrence and severity of windthrows, with plateau and slopes being affected more often and severely than valleys (Everham & Brokaw, 1996; Marra et al., 2014; Rifai et al., 2016).

While our models can predict the trajectory of biomass change after windthrow, we cannot assess the effects of windthrows on forest and carbon dynamics at larger spatial scales without more information on the size distribution and return frequency of windthrows at the landscape level. We have selected our transects to span gradients of windthrow severity, but their non-random positions do not allow us to make any inferences on the relative area made up by windthrows of different age. If precise maps of return frequency and severity of windthrows existed, the relationships we uncovered could be applied to assess the consequences of windthrows on the regional biomass carbon budget.

Large-scale windthrows occur at low frequencies (i.e., centuries to thousands of years) (Espírito-Santo et al., 2010; Negrón-Juárez et al., 2018). Our data cover a continuous gradient of windthrow

sizes (from ~400 m^2 up to a several hectares) and tree-mortality severities. Therefore, the patterns we found are likely to represent the processes operating in smaller and more frequently occurring windthrows (i.e., on decadal to century scales; Chambers et al., 2013). As mentioned before, it is possible that the smaller windthrows (~400 m^2) we studied can occur on average every 74 years (Chambers et al., 2013). From this, it can be calculated that at equilibrium conditions 35% of the landscape would have been affected by a small-scale windthrow within the last 30 years (Supporting Information Figure S1a). This corresponds to the observation period covered by our chronosequence. According to our data, this fraction of forest landscape would thus still be dominated by light-wooded tree species forming forests that have not yet fully recovered their pre-disturbance biomass. Likewise, 18% of the landscape would be covered by forests disturbed within the last 10 years and exhibiting substantially reduced carbon stocks. It is thus conceivable that the legacy of windthrows may reduce the landscape carbon stocks considerably.

Future work needs to be devoted to characterizing the extent, the frequency, and the severity of wind disturbances at the basin scale. This is even more important as the wind disturbance regime is likely to be altered by climate change as a consequence of shifts in rainfall and convective systems (IPCC, 2014; Mcdowell et al., 2018; Tan, Jakob, Rossow, & Tselioudis, 2015). As of now, our analysis suggests that the carbon stocks of Central Amazon forests exhibit a high degree of resilience against windthrows when compared with human disturbances. However, disturbances that recur over a short time interval are likely to reduce the resilience and carbon storage capacity of tropical forests (Chazdon, 2014; Jakovac et al., 2015; Mesquita et al., 2015). Should climate change intensify the wind disturbance regime in the Amazon region such that windthrows recur more frequently (i.e., <40 years), substantial and long-lasting changes in biomass patterns and functional composition of forests can be expected. Shorter recurrence intervals between windthrows may eventually prevent these forests to return to old-growth levels of biomass and wood density and will divert them to alternate stable states dominated by pioneers with reduced carbon stocks.

ACKNOWLEDGMENTS

We are grateful to various members of the *Laboratório de Manejo Florestal* from the *Instituto Nacional de Pesquisas da Amazônia* (LMF/INPA) for their continuous support, in special to Francisco Q. Reis and Vilany M. C. Carneiro for their contribution on the species identification. We thank the *Superintendência da Zona Franca de Manaus* (SUFRAMA) for allowing us to access the roads *Ramal-ZF2* (part of the *Site 1*) and *Ramal-ZF5* (*Site 2*). We also thank the *Comunidade Tumbira*, the *Centro Estadual de Unidades de Conservação* and the *Secretaria de Estado do Meio Ambiente e Desenvolvimento Sustentável do Amazonas* (CEUC/SDS), and the *Instituto de Proteção Ambiental do Amazonas* (IPAAM) for allowing our study at the *Reserva de Desenvolvimento Sustentável do Rio Negro* (*Site 3*). We acknowledge Douglas Sheil, Bruno Hérault and four anonymous reviewers for their constructive comments on previous versions of this manuscript. RINJ and JQC were supported as part of the Next Generation Ecosystem Experiments-Tropics, funded by the U.S. Department of Energy, Office of Science, Office of Biological and Environmental Research.

ORCID

Daniel Magnabosco Marra http://orcid.org/0000-0003-1216-2982

REFERENCES

Adams, J. B., & Gillespie, A. R. (2006). *Remote sensing of landscapes with spectral images: a physical modeling approach*. Cambridge: Cambridge University Press.

Araujo, R. F., Nelson, B. W., Celes, C. H. S., & Chambers, J. Q. (2017). Regional distribution of large blowdown patches across Amazonia in 2005 caused by a single convective squall line. *Geophysical Research Letters*, *44*, 1–6. https://doi.org/10.1002/2017GL073564

Baker, T. R., Phillips, O. L., Malhi, Y., Almeida, S., Arroyo, L., Di Fiore, A., ... Martínez, R. V. (2004). Variation in wood density determines spatial patterns in Amazonian forest biomass. *Global Change Biology*, *10*(5), 545–562. https://doi.org/10.1111/j.1365-2486.2004.00751.x

Bellingham, P., Tanner, E., & Healey, J. (1994). Sprouting of trees in Jamaican montane forests, after a Hurricane. *Journal of Ecology*, *82*(4), 747–758. https://doi.org/10.2307/2261440

Braga, P. I. S. (1979). Subdivisão fitogeográfica, tipos de vegetação, conservação e inventário florístico da floresta amazônica. *Acta Amazonica*, *9*(4), 53–80. https://doi.org/10.1590/1809-43921979094s053

Breiman, L. (2001). Random forests. *Machine Learning*, *45*(1), 5–32.

Burslem, D., & Whitmore, T. C. (1999). Species diversity, susceptibility to disturbance and tree population dynamics in tropical rain forest. *Journal of Vegetation Science*, *10*(6), 767–776. https://doi.org/10.2307/3237301

Burslem, D., Whitmore, T., & Brown, G. (2000). Short-term effects of cyclone impact and long-term recovery of tropical rain forest on Kolombangara, Solomon Islands. *Journal of Ecology*, *88*(6), 1063–1078. https://doi.org/10.1046/j.1365-2745.2000.00517.x

Canham, C. D., Thompson, J., Zimmerman, J. K., & Uriarte, M. (2010). Variation in susceptibility to hurricane damage as a function of storm intensity in Puerto Rican tree species. *Biotropica*, *42*(1), 87–94. https://doi.org/10.1111/j.1744-7429.2009.00545.x

Chambers, J. Q., Asner, G. P., Morton, D. C., Anderson, L. O., Saatchi, S. S., Espírito-Santo, F. D. B., ... Souza, C. Jr (2007). Regional ecosystem structure and function: Ecological insights from remote sensing of tropical forests. *Trends in Ecology & Evolution*, *22*(8), 414–423. https://doi.org/10.1016/j.tree.2007.05.001

Chambers, J. Q., Higuchi, N., Schimel, J. P., Ferreira, L. V., & Melack, J. M. (2000). Decomposition and carbon cycling of dead trees in tropical forests of the central Amazon. *Oecologia*, *122*(3), 380–388. https://doi.org/10.1007/s004420050044

Chambers, J. Q., Negron-Juarez, R. I., Marra, D. M., Di Vittorio, A., Tews, J., Roberts, D., ... Higuchi, N. (2013). The steady-state mosaic of disturbance and succession across an old-growth Central Amazon forest landscape. *Proceedings of the National Academy of Sciences of the United States of America*, *110*(10), 3949–3954. https://doi.org/10.1073/pnas.1202894110

Chambers, J. Q., Robertson, A. L., Carneiro, V. M. C., Lima, A. J. N., Smith, M. L., Plourde, L. C., & Higuchi, N. (2009). Hyperspectral remote detection of niche partitioning among canopy trees driven by blowdown gap disturbances in the Central Amazon. *Oecologia*, *160*(1), 107–117. https://doi.org/10.1007/s00442-008-1274-9

Chave, J., Coomes, D., Jansen, S., Lewis, S. L., Swenson, N. G., & Zanne, A. E. (2009). Towards a worldwide wood economics spectrum. *Ecology Letters*, *12*(4), 351–366. https://doi.org/10.1111/j.1461-0248.2009.01285.x

Chazdon, R. (2014). *Second growth: the promise of tropical forest regeneration in an age of deforestation*. Chicago, IL: University of Chicago Press.

Clark, D. B., & Clark, D. A. (2000). Landscape-scale variation in forest structure and biomass in a tropical rain forest. *Forest Ecology and Management*, *137*(1–3), 185–198. https://doi.org/10.1016/S0378-1127(99)00327-8

Curran, T. J., Brown, R. L., Edwards, E., Hopkins, K., Kelley, C., McCarthy, E., ... Wolf, J. (2008). Plant functional traits explain interspecific differences in immediate cyclone damage to trees of an endangered rainforest community in north Queensland. *Austral Ecology*, *33*(4), 451–461. https://doi.org/10.1111/j.1442-9993.2008.01900.x

Cutler, D. R., Edwards, T. C., Beard, K. H., Cutler, A., Hess, K. T., Gibson, J., & Lawler, J. J. (2007). Random forests for classification in ecology. *Ecology*, *88*(11), 2783–2792. https://doi.org/10.1890/07-0539.1

da Silva, R. P., dos Santos, J., Tribuzy, E. S., Chambers, J. Q., Nakamura, S., & Higuchi, N. (2002). Diameter increment and growth patterns for individual tree growing in Central Amazon, Brazil. *Forest Ecology and Management*, *166*(1–3), 295–301. https://doi.org/10.1016/S0378-1127(01)00678-8

de Castilho, C. V., Magnusson, W. E., de Araújo, R. N. O., & Luizão, F. J. (2010). Short-term temporal changes in tree live biomass in a Central Amazonian forest, Brazil. *Biotropica*, *42*(1), 95–103. https://doi.org/10.1111/j.1744-7429.2009.00543.x

de Oliveira, M., Higuchi, N., Celes, C., & Higuchi, F. (2014). Size of plots and forms for forest inventory of tree species in Central Amazon. *Ciência Florestal*, *24*(3), 645–653.

de Oliveira, A. A., & Mori, S. A. (1999). A central Amazonian terra firme forest. I. High tree species richness on poor soils. *Biodiversity and Conservation*, *8*(9), 1219–1244.

de Toledo, J. J., Magnusson, W. E., Castilho, C. V., & Nascimento, H. E. M. (2011). How much variation in tree mortality is predicted by soil and topography in Central Amazonia? *Forest Ecology and Management*, *262*(3), 331–338.

dos Santos, L. T., Magnabosco Marra, D., Trumbore, S., De Camargo, P. B., Negrón-Juárez, R. I., Lima, A. J. N., ... Higuchi, N. (2016). Windthrows increase soil carbon stocks in a central Amazon forest. *Biogeosciences*, *13*(4), 1299–1308. https://doi.org/10.5194/bg-13-1299-2016

Espírito-Santo, F. D. B., Gloor, M., Keller, M., Malhi, Y., Saatchi, S., Nelson, B., ... Phillips, O. L. (2014). Size and frequency of natural forest disturbances and the Amazon forest carbon balance. *Nature Communications*, *5*(3434), 1–6.

Espírito-Santo, F. D. B., Keller, M., Braswell, B., Nelson, B. W., Frolking, S., & Vicente, G. (2010). Storm intensity and old-growth forest disturbances in the Amazon region. *Geophysical Research Letters*, *37*(11), 1–6. https://doi.org/10.1029/2010GL043146

Everham, E. M., & Brokaw, N. V. L. (1996). Forest damage and recovery from catastrophic wind. *The Botanical Review*, *62*(2), 113–185. https://doi.org/10.1007/BF02857920

Fauset, S., Johnson, M. O., Gloor, M., Baker, T. R., Monteagudo, M. A., Brienen, R. J. W., ... Phillips, O. L. (2015). Hyperdominance in Amazonian forest carbon cycling. *Nature Communications*, *6*, 6857.

Fearnside, P. M. (1997). Wood density for estimating forest biomass in Brazilian Amazonia. *Forest Ecology and Management*, *90*, 59–87. https://doi.org/10.1016/S0378-1127(96)03840-6

Galbraith, D., Malhi, Y., Affum-Baffoe, K., Castanho, A. D. A., Doughty, C. E., Fisher, R. A., ... Lloyd, J. (2013). Residence times of woody biomass in tropical forests. *Plant Ecology & Diversity*, *6*(1), 139–157. https://doi.org/10.1080/17550874.2013.770578

Garstang, M., White, S., Shugart, H. H., & Halverson, J. (1998). Convective cloud downdrafts as the cause of large blowdowns in the Amazon rainforest. *Meteorology and Atmospheric Physics*, *67*(1–4), 199–212. https://doi.org/10.1007/BF01277510

Gloor, M., Phillips, O. L., Lloyd, J. J., Lewis, S. L., Malhi, Y., Baker, T. R., ... van der Heijden, G. (2009). Does the disturbance hypothesis explain the biomass increase in basin-wide Amazon forest plot data? *Global Change Biology*, *15*(10), 2418–2430.

Goulamoussène, Y., Bedeau, C., Descroix, L., Linguet, L., & Hérault, B. (2017). Environmental control of natural gap size distribution in tropical forests. *Biogeosciences*, *14*, 353–364. https://doi.org/10.5194/bg-14-353-2017

Hastie, T. J. T., & Tibshirani, R. J. (1990). *Generalized additive models. Statistics (Vol. 1)*. New York: Chapman and Hall/CRC.

Hérault, B., Beauchêne, J., Muller, F., Wagner, F., Baraloto, C., Blanc, L., & Martin, J. M. (2010). Modeling decay rates of dead wood in a neotropical forest. *Oecologia*, *164*(1), 243–251. https://doi.org/10.1007/s00442-010-1602-8

Hérault, B., & Piponiot, C. (2018). Key drivers of ecosystem recovery after disturbance in a neotropical forest. *Forest Ecosystems*, *5*(1), 2. https://doi.org/10.1186/s40663-017-0126-7

Higuchi, N., dos Santos, J., Ribeiro, R. J., Minette, L., & Biot, Y. (1998). Biomassa da parte aérea da vegetação da floresta tropical úmida de terra-firme da Amazônia brasileira. *Acta Amazonica*, *28*(2), 153–166. https://doi.org/10.1590/1809-43921998282166

Hjerpe, J., Hedenâs, H., & Elmqvist, T. (2001). Tropical rain forest recovery from cyclone damage and fire in Samoa. *Biotropica*, *33*(2), 249–259.

IPCC (2014). Climate Change 2014: Synthesis Report. Contribution of Working Groups I, II and III to the Fifth Assessment Report of the Intergovernmental Panel on Climate Change. Geneva, Switzerland. Retrieved from https://www.ipcc.ch/report/ar5/syr/.

Jakovac, C. C., Peña-Claros, M., Kuyper, T. W., & Bongers, F. (2015). Loss of secondary-forest resilience by land-use intensification in the Amazon. *Journal of Ecology*, *103*, 67–77. https://doi.org/10.1111/1365-2745.12298

Johnson, M., Galbraith, D., Gloor, E., De Deurwaerder, H., Guimberteau, M., Rammig, A., ... Baker, T. R. (2016). Variation in stem mortality rates determines patterns of aboveground biomass in Amazonian forests: Implications for dynamic global vegetation models. *Global Change Biology*, *22*(12), 3996–4013. https://doi.org/10.1111/gcb.13315

King, D. A. (1996). Allometry and life history of tropical trees. *Journal of Tropical Ecology*, *12*, 25–44. https://doi.org/10.1017/S0266467400009299

Laurance, W., & Curran, T. (2008). Impacts of wind disturbance on fragmented tropical forests: A review and synthesis. *Austral Ecology*, *33*(4), 399–408. https://doi.org/10.1111/j.1442-9993.2008.01895.x

Laurance, W., Nascimento, H., Laurance, S., Andrade, A., Fearnside, P., Ribeiro, J., & Capretz, R. (2006). Rain forest fragmentation and the proliferation of successional trees. *Ecology*, *87*(2), 469–482. https://doi.org/10.1890/05-0064

Laurance, W. F., Nascimento, H. E. M., Laurance, S. G., Condit, R., D'Angelo, S., & Andrade, A. (2004). Inferred longevity of Amazonian rainforest trees based on a long-term demographic study. *Forest Ecology and Management*, *190*(2–3), 131–143. https://doi.org/10.1016/j.foreco.2003.09.011

Lugo, A. E. (2008). Visible and invisible effects of hurricanes on forest ecosystems: An international review. *Austral Ecology*, *33*, 368–398.

Lugo, A. E., & Scatena, F. N. (1996). Background and catastrophic tree mortality in tropical moist, wet, and rain forests. *Biotropica*, *28*(4), 585–599. https://doi.org/10.2307/2389099

Magnabosco Marra, D., Higuchi, N., Trumbore, S. E., Ribeiro, G. H. P. M., Dos Santos, J., Carneiro, V. M. C., ... Wirth, C. (2016). Predicting biomass of hyperdiverse and structurally complex central Amazonian

forests - A virtual approach using extensive field data. *Biogeosciences*, *13*(5), 1553–1570.

Magnabosco Marra, D. (2016). Effects of windthrows on the interaction between tree species composition, forest dynamics and carbon balance in Central Amazon. PhD thesis, University of Leipzig, Leipzig. Retrieved from https://pure.mpg.de/pubman/faces/ViewItemOverviewPage.jsp?itemId=item_2424147) be mentioned?

Marra, D., Chambers, J., Higuchi, N., Trumbore, S., Ribeiro, G., Dos Santos, J., … Wirth, C. (2014). Large-scale wind disturbances promote tree diversity in a central Amazon forest. *PLoS One*, *9*(8), e103711–e103711. https://doi.org/10.1371/journal.pone.0103711

Mascaro, J., Perfecto, I., Barros, O., Boucher, D. H., de la Cerda, I. G., Ruiz, J., & Vandermeer, J. (2005). Aboveground biomass accumulation in a tropical wet forest in Nicaragua following a catastrophic hurricane disturbance. *Biotropica*, *37*(4), 600–608.

Mazzei, L., Sist, P., Ruschel, A., Putz, F. E., Marco, P., Pena, W., & Ferreira, J. E. R. (2010). Above-ground biomass dynamics after reduced-impact logging in the Eastern Amazon. *Forest Ecology and Management*, *259*(3), 367–373. https://doi.org/10.1016/j.foreco.2009.10.031

Mcdowell, N., Allen, C. D., Anderson-Teixeira, K., Brando, P., Brienen, R., Chambers, J., … Xu, X. (2018). Drivers and mechanisms of tree mortality in moist tropical forests. *New Phytologist*, *219*, 851–869. https://doi.org/10.1111/nph.15027

Mesquita, R. D. C. G., Massoca, P. E. D. S., Jakovac, C. C., Bentos, T. V., & Williamson, G. B. (2015). Amazon rain forest succession: Stochasticity or land-use legacy? *BioScience*, *65*(9), 849–861. https://doi.org/10.1093/biosci/biv108

Mitchell, S. (2013). Wind as a natural disturbance agent in forests: A synthesis. *Forestry*, *86*(2), 147–157.

Nascimento, H. E. M., & Laurance, W. F. (2004). Biomass dynamics in Amazonian forest fragments. *Ecological Applications*, *14*(4), 127–138. https://doi.org/10.1890/01-6003

Negrón-Juárez, R. I., Chambers, J. Q., Guimaraes, G., Zeng, H., Raupp, C. F. M., Marra, D. M., … Higuchi, N. (2010). Widespread Amazon forest tree mortality from a single cross-basin squall line event. *Geophysical Research Letters*, *37*(16), 1–5. https://doi.org/10.1029/2010GL043733

Negrón-Juárez, R. I., Chambers, J. Q., Marra, D. M., Ribeiro, G. H. P. M., Rifai, S. W., Higuchi, N., & Roberts, D. (2011). Detection of subpixel treefall gaps with Landsat imagery in Central Amazon forests. *Remote Sensing of Environment*, *115*(12), 3322–3328. https://doi.org/10.1016/j.rse.2011.07.015

Negrón-Juárez, R. I., Holm, J., Magnabosco Marra, D., Rifai, S., Riley, W., Chambers, J., … Higuchi, N. (2018). Vulnerability of Amazon forests to storm-driven tree mortality. *Environmental Research Letters*, *13*(5), 054021. https://doi.org/10.1088/1748-9326/aabe9f

Negrón-Juárez, R. I., Jenkins, H. S., Raupp, C. F. M., Riley, W. J., Kueppers, L. M., Marra, D. M., Higuchi, N. (2017). Windthrow variability in Central Amazonia. *Atmosphere*, *8*(2), 28. https://doi.org/10.3390/atmos8020028

Nelder, J. A., & Wedderburn, R. W. M. (1972). Generalized linear models. *J. R. Statist. Soc. A.*, *135*(3), 370–384. https://doi.org/10.2307/2344614

Nelson, B. W., Kapos, V., Adams, J. B., Oliveira, W. J., & Braun, O. P. G. (1994). Forest disturbance by large blowdowns in the Brazilian Amazon. *Ecology*, *75*(3), 853–858. https://doi.org/10.2307/1941742

Nogueira, E. M., Fearnside, P. M., Nelson, B. W., & França, M. B. (2007). Wood density in forests of Brazil's 'arc of deforestation': Implications for biomass and flux of carbon from land-use change in Amazonia. *Forest Ecology and Management*, *248*, 119–135. https://doi.org/10.1016/j.foreco.2007.04.047

Nogueira, E. M., Nelson, B. W., & Fearnside, P. M. (2005). Wood density in a dense forest in central Amazonia. *Brazil. Forest Ecology and Management*, *208*(1–3), 261–286. https://doi.org/10.1016/j.foreco.2004.12.007

Putz, F. E. (1983). Treefall pits and mounds, buried seeds, and the importance of soil disturbance to pioneer trees on Barro Colorado Island, Panama. *Ecology*, *64*(5), 1069–1074. https://doi.org/10.2307/1937815

Putz, F. E., & Brokaw, N. V. L. (1989). Sprouting of broken trees on Barro Colorado Island, Panama. *Ecology*, *70*(2), 508–512. https://doi.org/10.2307/1937555

Ribeiro, G. H. P. M., Chambers, J. Q., Peterson, C. J., Trumbore, S. E., Magnabosco Marra, D., Wirth, C., … Higuchi, N. (2016). Mechanical vulnerability and resistance to snapping and uprooting for Central Amazon tree species. *Forest Ecology and Management*, *380*(380), 1–10. https://doi.org/10.1016/j.foreco.2016.08.039

Ribeiro, G. H. P. M., Suwa, R., Marra, D. M., Kajimoto, T., Ishizuka, M., Higuchi, N., … Higuchi, N. (2014). Allometry for juvenile trees in an Amazonian forest after wind disturbance. *Japan Agricultural Research Quarterly*, *48*(2), 213–219. https://doi.org/10.6090/jarq.48.213

Rifai, S. W., Urquiza Muñoz, J. D., Negrón-Juárez, R. I., Ramírez Arévalo, F. R., Tello-Espinoza, R., Vanderwel, M. C., … Bohlman, S. A. (2016). Landscape-scale consequences of differential tree mortality from catastrophic wind disturbance in the Amazon. *Ecological Applications*, *26*(7), 2225–2237. https://doi.org/10.1002/eap.1368

Rüger, N., Comita, L., Condit, R., Purves, D., Rosenbaum, B., Visser, M., … Wirth, C. (2018). Beyond the fast-slow continuum: Demographic dimensions structuring tropical tree community. *Ecology Letters*, *21*, 1075–1084.

Rutishauser, E., Baraloto, C., Blanc, L., Descroix, L., Sota, E. D., Kanashiro, M., … Finegan, B. (2015). Rapid tree carbon recovery in Amazonian logged forests. *Current Biology*, *25*(18), R787–R788.

Scalley, H. T., Scatena, F. N., Lugo, A. E., Moya, S., & Estrada Ruiz, C. R. (2010). Changes in structure, composition, and nutrients during 15 Years of hurricane-induced succession in a subtropical wet forest in Puerto Rico. *Biotropica*, *42*(4), 455–463.

Scatena, F. N., Moya, S., Estrada, C., & Chinea, J. D. (1996). The first five years in the reorganization of aboveground biomass and nutrient use following Hurricane Hugo in the Bisley Experimental Watersheds, Luquillo Experimental Forest, Puerto Rico. *Biotropica*, *28*(4), 424–440. https://doi.org/10.2307/2389086

Schwartz, N. B., Uriarte, M., DeFries, R., Bedka, K. M., Fernandes, K., Gutiérrez-Vélez, V., & Pinedo-Vasquez, M. A. (2017). Fragmentation increases wind disturbance impacts on forest structure and carbon stocks in a western Amazonian landscape. *Ecological Applications*, 1–15. https://doi.org/10.1002/eap.1576

Silvério, D. V., Brando, P. M., Bustamante, M. M. C., Putz, F., Magnabosco Marra D., Levick, S. R., & Trumbore, S. E. accepted. Fire, fragmentation, and windstorms: A recipe for tropical forest degradation. *Journal of Ecology*. https://doi.org/10.1111/1365-2745.13076

Swaine, M. D., & Whitmore, T. C. (1988). On the definition of ecological species groups in tropical rain forests. *Vegetatio*, *75*(1–2), 81–86. https://doi.org/10.1007/BF00044629

Talbot, J., Lewis, S. L., Lopez-Gonzalez, G., Brienen, R. J. W., Monteagudo, A., Baker, T. R., … Phillips, O. L. (2014). Methods to estimate aboveground wood productivity from long-term forest inventory plots. *Forest Ecology and Management*, *320*, 30–38. https://doi.org/10.1016/j.foreco.2014.02.021

Tan, J., Jakob, C., Rossow, W. B., & Tselioudis, G. (2015). Increases in tropical rainfall driven by changes in frequency of organized deep convection. *Nature*, *519*(7544), 451–454.

Vandermeer, J., & Cerda, I. G. (2004). Height dynamics of the thinning canopy of a tropical rain forest: 14 years of succession in a post-hurricane forest in Nicaragua. *Forest Ecology and Management*, *199*(1), 125–135. https://doi.org/10.1016/j.foreco.2004.05.033

Vandermeer, J., la Cerda, I. G., Boucher, D., Perfecto, I., & Ruiz, J. (2000). Hurricane disturbance and tropical tree species diversity. *Science (New York, N.Y.)*, *290*(5492), 788–791. https://doi.org/10.1126/science.290.5492.788

Vieira, S., de Camargo, P. B., Selhorst, D., da Silva, R., Hutyra, L., Chambers, J. Q., ... Martinelli, L. A. (2004). Forest structure and carbon dynamics in Amazonian tropical rain forests. *Oecologia*, *140*(3), 468–479. https://doi.org/10.1007/s00442-004-1598-z

Vitousek, P. M., & Denslow, J. S. (1986). Nitrogen and phosphorus availability in treefall gaps of a lowland tropical rainforest. *The Journal of Ecology*, *74*(4), 1167–1178. https://doi.org/10.2307/2260241

Wood, S. N. (2006). *Generalized additive models: An introduction with R*. Boca Raton, MA: Chapman and Hall/CRC.

Yih, K., Boucher, D. H., Vandermeer, J. H., & Zamora, N. (1991). Recovery of the rain forest of southeastern Nicaragua after destruction by hurricane Joan. *Biotropica*, https://doi.org/10.2307/2388295.

SUPPORTING INFORMATION

Additional supporting information may be found online in the Supporting Information section at the end of the article.

How to cite this article: Magnabosco Marra D, Trumbore SE, Higuchi N, et al. Windthrows control biomass patterns and functional composition of Amazon forests. *Glob Change Biol*. 2018;24:5867–5881. https://doi.org/10.1111/gcb.14457